Journal of Materials Chemistry C

PAPER

View Article Online
View Journal



Cite this: DOI: 10.1039/c4tc02232g

# The effects of heavy atoms on the exciton diffusion properties in photoactive thin films of tetrakis(4-carbomethoxyphenyl)porphyrins†

Angy L. Ortiz, Graham S. Collier, Dawn M. Marin, Jennifer A. Kassel, Reynolds J. Ivins, Nicholas G. Grubich and Michael G. Walter*

Received 6th October 2014
Accepted 30th November 2014

DOI: 10.1039/c4tc02232g

www.rsc.org/MaterialsC

The singlet exciton diffusion properties of solution-cast thin films prepared from mixed substituent monoiodophenyl or monobromophenyl derivatives of 5,10,15,20-tetrakis(4-carbomethoxyphenyl) porphyrin ($TCM_4PP$) were investigated for use in solar energy conversion applications. The photoluminescent singlet decay lifetime PL($t$) of pristine porphyrin films and films lightly doped (0.1–0.6% wt) with [6,6]-phenyl-C61-butryic acid methyl ester (PCBM) were used to obtain relative quenching efficiencies ($Q$). The exciton diffusion coefficient ($D$) and exciton diffusion length ($L_D$) for each derivative were obtained by modeling the quenching efficiency and PL lifetime decay data using a 3D exciton Monte Carlo diffusion simulation. Although the three TCMPP derivatives showed nearly identical absorbances and electrochemical properties, the monobromophenyl or monoiodophenyl substituted porphyrins exhibited significantly lower steady-state emission intensities and fluorescent lifetimes in solution. Amorphous thin films of the halogenated derivatives also exhibited a decrease in the PL decay lifetimes, relative quenching efficiencies, and reduced singlet exciton diffusion lengths. The singlet exciton diffusion length for $TCM_4PP$ was calculated to be 15 nm and decreased by 71% to 4.4 nm for $TCM_3IPP$ with the addition of a single iodo substituent. Photocurrent–voltage measurements of the derivatives in a PCBM bulk heterojunction device suggest that lowered exciton diffusion and enhanced singlet to triplet exciton conversion, due to the heavy atom effect, decreases photoconversion efficiency.

## Introduction

In photosynthesis, photoinduced excitation energy travels through coordinated light-harvesting chlorophyll molecules to reaction centers within femtoseconds (or picoseconds).[1–3] Rapid and coherent excitonic wave migration in these natural systems has motivated researchers to synthesize and examine new chlorophyll/porphyrin derivatives for use in artificial light-harvesting antenna assemblies such as porphyrin arrays, polymers, and metal–organic frameworks (MOFs).[4–6] A wide variety of porphyrin structures have been evaluated in solution-processable organic photovoltaic (OPV) devices including *meso*-substituted tetraphenylporphyrins (TPPs), which have demonstrated efficiencies in OPVs between 1–4%.[7–12] Enhanced light harvesting in solar conversion devices relies on developing materials with long exciton diffusion lengths that allow for dissociation of excited states into free-charge carriers at donor/acceptor interfaces before recombination.[13–18] To increase the probability of exciton dissociation, interfaces must lie within the exciton diffusion length (typically between 10–20 nm for many organic semiconductors).[18,19] Extending singlet exciton diffusion lengths has resulted in higher photocurrents and may ultimately eliminate the requirement of nanostructured donor–acceptor interfaces.[18–21] Alternatively, enhancing the singlet to triplet exciton conversion yield in the photoactive layer has been shown to increase photoconversion efficiency of organic solar cells,[22–24] presumably due to longer triplet exciton diffusion lengths.[25,26] Studies have shown that enhanced photocurrent can result from triplet-triplet energy transfer,[24] or through singlet fission where two triplets are generated from a single excitation resulting in external quantum efficiencies above 100%.[27,28] Therefore, the development of organic semiconductor materials and device architectures amenable to utilizing triplet state formation is of great interest for new solar energy conversion systems. Porphyrins are well known for their efficiency in generating long-lived triplet excited states through intersystem crossing (ISC), and are widely used to generate singlet oxygen for photodynamic therapy applications.[29–33] To improve intersystem crossing, heavy atoms including metals and halogens, are included in the porphyrin structure to encourage spin–orbit coupling and the formation of triplet excited states.[32,34–37] Using $TCM_4PP$ and mixed-substituent bromophenyl or iodophenyl $TXCM_3PP$ derivatives, we have

*Department of Chemistry, Burson 200, 9201 University City Blvd., Charlotte, NC 28223-0001, USA. E-mail: Michael.Walter@uncc.edu*

† Electronic supplementary information (ESI) available. See DOI: 10.1039/c4tc02232g

investigated how increasing the generation of triplet states in porphyrin thin films affects singlet exciton diffusion lengths and photocurrent efficiency. The singlet exciton diffusivity ($D$) and 3D diffusion length ($L_D$) was calculated using the PL lifetime decay measurements of pristine and PCBM acceptor-doped films. The thin films were prepared using three tetra-substituted porphyrins, including $TCM_4PP$, 5-(4-bromophenyl)-10,15,20-tris(4-carboxymethoxyphenyl)porphyrin ($TBCM_3PP$), and 5,10,15-tris(4-carboxymethoxyphenyl)-20-(iodophenyl)-porphyrin ($TCM_3IPP$). The monobromophenyl and mono-iodophenyl asymmetric porphyrin derivatives were synthesized using a mixed-pot synthesis under Adler–Longo conditions to obtain a mixture of statistical products.[38] These were separated using centrifugal chromatographic techniques to obtain high purity $TBCM_3PP$ and $TCM_3IPP$.[32,37] The work demonstrates for the first time how heavy atoms (halogens) affect singlet exciton diffusion in porphyrin thin films, the usefulness of a simple Monte Carlo random-walk diffusion model to calculate exciton $D$ and $L_D$ for these materials, and the implications of using brominated or iodinated porphyrin-based semiconductors in solar energy conversion devices.

# Experimental

### a. Materials and instrumentation

Materials for porphyrin syntheses and purification include 4-bromobenzaldehyde, 4-carbomethoxybenzaldehyde, 4-iodobenzaldehyde, propionic acid, and dichloromethane, all purchased from Sigma-Aldrich and used without further purification except pyrrole, which was distilled prior to use. Tetrahydrofuran, from Sigma Aldrich, was dried over activated 3 Å sieves to achieve an ultra-dry solvent, and stored under argon. Poly(3,4-ethylenedioxythiophene) poly(styrenesulfonate) (PEDOT:PSS) (Clevios AI4083) was obtained from Ossila and was filtered using 0.45 μm pore diameter cellulose acetate syringe filters prior to use. Centrifugal chromatography was performed on a Chromatotron (Model 7924T – Harrison Research, Inc.) using a 2 mm thick silica plate prepared using TLC grade silica (Aldrich). All $^1$H-NMR measurements were made on a JEOL 300 MHz NMR. UV-vis spectra were collected on a Cary 300 UV-vis spectrophotometer using THF for solution measurements. Fluorescence measurements and excited state lifetimes ($\tau_{fl}$) using time-correlated single photon counting (TCSPC) were taken on a Jobin Yvon-Spex Fluorolog equipped with a 341 nm diode laser. Fig. S4† shows steady-state PL quenching of $TBCM_3PP$ thin films with 1 : 2 and 1 : 4 PCBM by weight. Fig. S5† shows fluorescent lifetime decays and photophysical parameters of the derivatives in solution, which were degassed with 5 freeze–pump–thaw cycles (in dichloromethane). Thin-film PL decay measurements using TCSPC were taken on a Spectra Physics MaiTai, operating at 80 MHz equipped with a femtosecond Ti:Sapphire laser. Patterned tin-doped indium oxide (ITO) electrodes were obtained from Ossila, 18–20 Ω sq$^{-1}$. Film thickness was measured with a Dimension 3100 SPM System (AFM) with a Nanoscope IV controller. The XRD $\theta/2\theta$ patterns were obtained using a Panalytical X'Pert Pro MPD with Ni filtered Cu Kα radiation from a fixed anode at 45 kV, 40 mA. Data were collected within the range of $10^\circ < 2\theta < 120^\circ$ with a 0.02° step size, and a counting time of 0.35 s per point in all cases.

### b. Preparation of porphyrin derivatives

**5,10,15,20-Tetrakis(4-carbomethoxyphenyl)porphyrin ($TCM_4PP$).** $TCM_4PP$ was obtained using previously reported methods.[38]

**5-(4-Bromophenyl)-10,15,20-tris(4-carbomethoxyphenyl)-porphyrin ($TBCM_3PP$).** Distilled pyrrole (1.127 mL, 0.016 mol) was added dropwise over 15 min to a stirring solution of 4-carbomethoxybenzaldehyde (2.00 g, 0.012 mol) and 4-bromobenzaldehyde (0.7513 g, 0.004 mol) in 150 mL of propionic acid and was refluxed for 30 min. The reaction mixture sat overnight, was filtered and washed with cold methanol, yielding a purple solid (0.410 g of the mixed porphyrin, 12%). The mono-bromophenylporphyrin was purified by preparatory TLC or centrifugal chromatography using a 1 : 1 gradient of DCM : hexanes. The 4th band, on TLC or the Chromatotron, was determined to be $TBCM_3PP$. $^1$H NMR (300 MHz, $CDCl_3$, TMS, $\delta$): 8.81 (m, β-pyrrole protons, 8H), 8.44 (d, $J = 7.7$ Hz, 6H), 8.28 (d, $J = 8.1$ Hz, 6H), 8.06 (d, $J = 8.4$ Hz, 2H), 7.89 (d, $J = 8.4$ Hz, 2H), 4.11 (s, 9H), −2.82 (s, 2H) UV-vis $\lambda_{max}$ (THF, $\varepsilon = M^{-1}$ cm$^{-1}$): 418 nm ($\varepsilon = 442\,000$), 514 nm ($\varepsilon = 20\,000$), 548 nm ($\varepsilon = 9000$), 592 nm ($\varepsilon = 6000$), 648 nm ($\varepsilon = 2000$) Mass Spec. MALDI-TOF (calcd for $C_{50}H_{35}BrN_4O_6$: 867.74 found: M + 2 = 869.53).

**5,10,15-Tris(4-carboxymethoxyphenyl)-20-(iodophenyl)-porphyrin ($TCM_3IPP$).** Distilled pyrrole (0.607 mL, 8.75 mmol) was added dropwise over 15 min to a stirring solution of 4-carbomethoxybenzaldehyde (1.08 g, 6.56 mmol) and 4-iodobenzaldehyde (0.573 g, 2.19 mmol) in 100 mL of propionic acid and was refluxed for 30 min. After sitting overnight, the reaction mixture was filtered and washed with methanol, yielding a purple solid (0.221 g of mixed porphyrins, 11%). The mono-iodophenyl porphyrin was purified by preparatory TLC or centrifugal chromatography with a Chromatotron using a 1 : 1 gradient of DCM : hexanes. The 4th band was collected and determined to be $TCM_3IPP$. $^1$H NMR (300 MHz, $CDCl_3$, TMS, $\delta$): 8.85 (s, 1H), 8.84 (s, 1H), 8.81 (m, β-pyrrole protons, 6H), 8.43 (d, $J = 8.4$ Hz, 6H). 8.28 (d, $J = 8.1$ Hz, 6H), 8.08 (d, $J = 8.1$ Hz, 2H), 7.91 (d, $J = 8.1$ Hz, 2H), 4.11 (s, 9H), −2.83 (s, 2H) UV-vis $\lambda_{max}$ (THF, $\varepsilon = M^{-1}$ cm$^{-1}$): 418 nm ($\varepsilon = 458\,000$), 514 nm ($\varepsilon = 21\,000$), 549 nm ($\varepsilon = 9000$), 591 nm ($\varepsilon = 6000$), 646 nm ($\varepsilon = 4000$) MALDI-TOF (calcd for $C_{50}H_{35}IN_4O_6$: 914.16 found: M + 1 = 915.0).

### c. Porphyrin thin-film preparation and characterization

Microscope slides were cleaned by consecutive sonication with detergent, acetone and isopropyl alcohol, and then dried by purging with $N_2$. Finally they were placed in a UV-ozone cleaner for 10 min. Stock solutions of $TCM_4PP$ (9 mM), $TBCM_3PP$ (4 mM), $TCM_3IPP$ (4 mM) and PCBM (0.13 mM) in chlorobenzene (CB) were prepared and heated to 70 °C. Porphyrin solutions were doped with varying amounts of PCBM to obtain a range of 0.1–0.6 wt% PCBM, which is equivalent to 0.033–0.2% PCBM volume fraction ($v_{frac}$).

 

Inside a $N_2$ filled glovebox, each solution was spin-coated onto a glass substrate to produce a ~20 nm thick film of porphyrin : PCBM blend. Prior to photophysical measurements, films were encapsulated with a coverslip and sealed with epoxy to avoid photobleaching. The PCBM $v_{frac}$ is the ratio of the total volume occupied by PCBM molecules ($V_{PCBM}$) *versus* the blend volume. Thus, $v_{frac}$ is related to the concentration of PCBM ($C_{PCBM}$) in the blend by the eqn (1):[39]

$$v_{frac} = C_{PCBM} V_{PCBM} \quad (1)$$

$$V_{PCBM} = \frac{4}{3}\pi r^3, \quad (2)$$

$$C_{PCBM} = \frac{\rho_{PCBM}}{M_{PCBM}} N_A, \quad (3)$$

where, $r$ is the radius of PCBM, $M_{PCBM}$ is the molar mass of PCBM, $N_A$ is the Avogadro constant and $\rho_{PCBM}$ is the density of PCBM. The density of PCBM in the blend is related by the mass fraction of PCBM as:[39]

$$m_{frac} = \frac{\rho_{PCBM}}{\rho_{PCBM} + \rho_{porphyrin}} \quad (4)$$

Porphyrin densities ($\rho_{porphyrin}$) were experimentally found to be 0.97 g $cm^{-3}$. The PL decay of each film was measured by a laser repetition rate of laser 200 kHz and excited at 440 nm. The PL decays were fitted using Igor Pro 6.3 software. The fitted PL decays were simulated by Monte Carlo eDiffusion Software to obtain exciton diffusion coefficients ($D$).[39]

### d. OPV device fabrication and characterization

Patterned tin-doped indium oxide electrodes (ITO – resistance ~18–20 Ω $sq^{-1}$) were cleaned by consecutive sonication in 0.2 M sodium hydroxide (NaOH), acetone and isopropyl alcohol. Electrodes were rinsed with Milli-Q water after every sonication cycle, dried with $N_2$ and placed in a UV-ozone cleaner for 15 min. PEDOT:PSS was deposited onto a clean ITO surface through spin-coating. Stock solutions of $TCM_4PP$ (10 mM), $TBCM_3PP$ (20 mM), $TCM_3IPP$ (20 mM) and PCBM (23 mM) in chlorobenzene (CB) were prepared and heated to 70 °C prior to use. Each stock porphyrin solution was mixed with PCBM in a weight ratio 1 : 4 (porphyrin : PCBM) at a 20 mg $mL^{-1}$ concentration. The porphyrin : PCBM active layer was deposited using spin-coat deposition in an $N_2$ glovebox environment followed by BPhen (8 nm) and aluminum contact (100 nm) deposition under vacuum ($10^{-6}$ mbar). The architectural structure of the final device was ITO/PEDOT:PSS/Porphyrin : PCBM/BPhen/Al. *J–V* data were obtained using a Keithley 236 source-measure controlled by LabView software. Illumination was provided by a Newport 300 W Xenon lamp with an AM1.5 solar spectrum filter that was calibrated with a Si photodiode to produce an illumination of 100 mW $cm^{-2}$ of AM1.5 G illumination (1 sun illumination).

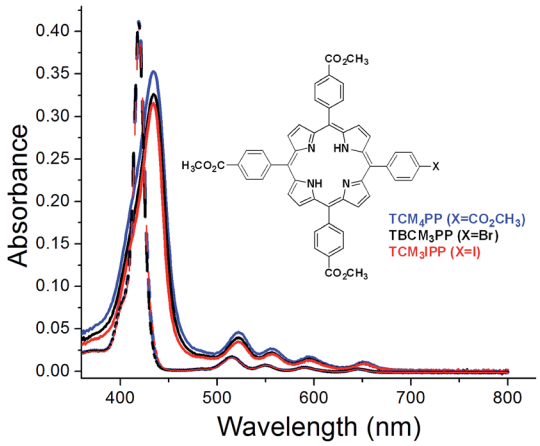


Fig. 1 Absorption spectra of solutions (6 μM) (a) $TCM_4PP$ (--), $TBCM_3PP$ (--) and $TCM_3IPP$ (--) and films (b) $TCM_4PP$ (–), $TBCM_3PP$ (–) and $TCM_3IPP$ (–). Film thickness: 20 nm.

## Results and discussion

### a. Solution/thin film absorption spectroscopy

The absorption spectra for solutions and pristine thin films of $TCM_4PP$, $TBCM_3PP$ and $TCM_3IPP$ are shown in Fig. 1. Solution UV-vis spectra of the three derivatives have identical molar absorptivities and absorption peaks in the Soret band at 418 nm ($\varepsilon = 450 \times 10^3$ $M^{-1}$ $cm^{-1}$) along with four Q bands spanning the visible region (514, 548, 591, and 646 nm), $Q_4$, $Q_3$, $Q_2$, and $Q_1$ respectively. A 16 nm red-shift and broadening of the Soret band (from 418 nm to 434 nm) is observed in the neat film UV-vis spectra (Fig. 1). This red-shift is indicative of energy level shifts caused by porphyrin stacking, while the broadening of the Soret band is attributed to the increase of the π–π interactions as a result of porphyrin stacking in thin films.[38,40]

### b. Exciton diffusion coefficient ($D$) and diffusion length ($L_D$)

Excitons are coulombically bound electron–hole pairs with a large binding energy, between 250–500 meV.[19,20] Exciton diffusion length $L_D$ is an important criterion for an organic semiconductor because of its influence on the probability of exciton dissociation. To efficiently dissociate a photoexcited state, an interface with an electron or hole acceptor with intrinsic energy levels that are sufficiently offset, is needed. Excitons must arrive at this interface before electron–hole recombination.[19–21] Several methods have been used to measure $L_D$ such as PL surface quenching, exciton–exciton annihilation, modeling of solar cell photocurrent spectra, time-resolved microwave conductivity, spectrally resolved PL quenching, and Förster resonance energy transfer theory.[41] Another recently developed technique is time-resolved PL bulk quenching modeled with a Monte Carlo eDiffusion computational simulation. This technique is convenient, fast and versatile for moderately crystalline and amorphous small molecule materials.[39,41–43] The simulation models non-interacting excitons randomly hopping in an intimately mixed material:quencher blend until they reach a quenching site. PCBM used as a quencher is modeled as a non-overlapping, homogeneous sphere of 0.5 nm radius randomly

placed into a simulation box of 50 × 50 × 50 nm. This box is considered to be a continuous medium of the donor material phase.[45] The inputs of the Monte Carlo eDiffusion simulation are the sample morphology, the measured PL decay lifetimes of the pristine material film and the material:quencher film, and the quencher volume fraction in that sample. The only fitting parameter and output parameter is the exciton diffusion coefficient ($D$). The simulation is repeated until the modeled and experimental PL decays converge, resulting in the calculated $D$ value.

According to the Einstein–Smoluchowski diffusion theory, $D$ is calculated as 1/6th times the quotient of the distance traveled by an exciton squared ($\delta s^2$) and the time interval for that iteration ($\delta t$). Each iteration models an exciton moving in a random 3D direction for a fixed distance $\delta s$ (eqn (6)) Finally, $L_D$ is defined as the root mean squared of the product of $D$, the average lifetime ($\tau$) and dimensionality ($a$ = 3 or 6) of the diffusion process (eqn (7)).[39]

$$D = \frac{\delta s^2}{6\delta t} \quad (5)$$

$$L_D = \sqrt{aD\tau} \quad (6)$$

Fig. 2 presents the measured PL lifetime decays for the neat films of $TCM_4PP$ (Fig. 2a), $TBCM_3PP$ (Fig. 2b) and $TCM_3IPP$ (Fig. 2c) and their blends doped with 0.06% and 0.2% PCBM volume fraction. It can be observed that the PL lifetime decays of the neat films follows the trend: $TCM_4PP$ (2.46 ns) > $TBCM_3PP$ (1.85 ns) > $TCM_3IPP$ (0.49 ns). These decays are in agreement with the observed fluorescence emission lifetime trends of the derivatives in solution with PL lifetimes observed for the derivatives: $TCM_4PP$ (8.52 ns), $TBCM_3PP$ (5.02 ns), and $TCM_3IPP$ (2.34 ns) (Fig. S5†). The addition of PCBM in the films also shortens the PL decay time, which is a result of the diffusion-limited exciton quenching at the porphyrin : PCBM bulk interface. A higher quenching is observed for $TCM_4PP$ (Fig. 2a) compared to $TBCM_3PP$ (Fig. 2b). The quenching for $TCM_3IPP$ (Fig. 2c) is almost negligible at 0.06% PCBM and increases with doping of 0.2% PCBM. The PL decays were modeled by Monte Carlo eDiffusion simulations to obtain $D$ values of $1.8 \times 10^{-4}$, $0.79 \times 10^{-4}$ and $0.73 \times 10^{-4}$ $cm^2\ s^{-1}$ that correspond to average $L_D$ values of 15, 9.4 and 4.4 nm in $TCM_4PP$, $TBCM_3PP$, and $TCM_3IPP$s respectively (Table 1). Exciton diffusion properties in tetraphenylporphyrin derivatives are dependant upon peripheral alkyl substituents and molecular orientation. For example, compared to *meso*-tetraphenylporphyrin ($H_2TPP$), the presence of ethyl substituents ($H_2TEPP$) increases $D$ and $L_D$ from $2 \times 10^{-5}$ $cm^2\ s^{-1}$ and 0.7 nm to $7 \times 10^{-4}$ $cm^2\ s^{-1}$ and 7.5 nm, respectively. The increase of $D$ and $L_D$ was attributed to a decrease in H-aggregates within the $H_2TEPP$ films.[40,44–48] The similarity in $D$ and $L_D$ values obtained in this study indicates that the $TCM_4PP$ films tested are similarly disordered and do not form H-aggregates. This is also in agreement with the absence of crystallinity observed in the X-ray diffraction of the thin films (Fig. S2†).

Another important parameter is the relative quenching efficiency ($Q$), which is defined as:

$$Q = 1 - \frac{\int \mathrm{PL}_{\mathrm{blend}}\,dt}{\int \mathrm{PL}_{\mathrm{pristine}}\,dt} \quad (7)$$

where, $PL_{blend}$ and $PL_{pristine}$ are decay profiles of a material:PCBM blend and pristine material, respectively. Eqn (7) indicates that if $Q \approx 0$, exciton quenching is insignificant (low concentrations of quenchers or poor exciton diffusivity). If $Q \approx 1$ (high PCBM concentrations or efficient exciton diffusion) and is accompanied by a considerably shortened lifetime, an effective quenching mechanism operates within the photoactive layer.[39,49] Table 1 lists the $\tau_{s1}$, $\tau_Q$, $Q$, $D$, $L_D$ values for $TCM_4PP$, $TBCM_3PP$ and $TCM_3IPP$. Although the PCBM volume fraction and molar absorptivities are the same in the three samples, $Q$ changes significantly from film to film. PCBM quenching in the $TBCM_3PP$ film is reduced compared to $TCM_4PP$ and it is even lower for the case of $TCM_3IPP$ ($L_D$ decreases 71% from $TCM_4PP$ to $TCM_3IPP$). These findings support a mechanism of shorter-

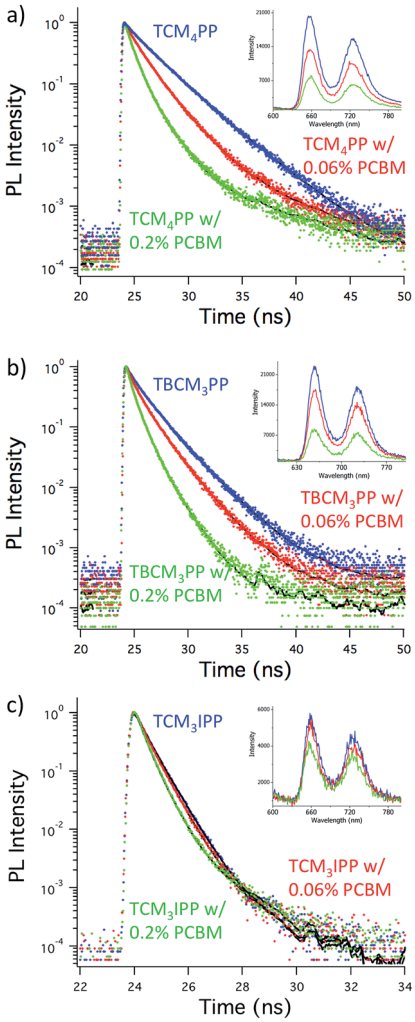


Fig. 2 Experimentally measured PL decays of pristine (a) $TCM_4PP$, (b) $TBCM_3PP$ and (c) $TCM_3IPP$ and their respective blends doped with 0.06% and 0.2% PCBM volume fraction. Inset: steady-state emission spectra of each film.

Table 1 Summary of: PL average lifetime decays ($\tau$), relative quenching efficiency ($Q$), exciton diffusion coefficient ($D$), diffusion length ($L_D$), $J_{sc}$ and $V_{oc}$ of $TCM_4PP$, $TBCM_3PP$ and $TCM_3IPP$

| | $\tau_{S1}$ (ns) | $\tau_Q$[a] (ns) | $Q$[a] | $D \times 10^{-4}$ cm$^2$ s$^{-1}$ | $L_D$ (nm) | $J_{sc}$[b] mA cm$^{-2}$ | $V_{oc}$[b] mV |
|---|---|---|---|---|---|---|---|
| $TCM_4PP$ | 2.46 ± 0.17 | 1.40 ± 0.16 | 0.363 ± 0.07 | 1.8 ± 0.6 | 15 ± 3.2 | 0.35 ± 0.01 | 489 ± 20 |
| $TBCM_3PP$ | 1.85 ± 0.04 | 1.48 ± 0.01 | 0.199 ± 0.02 | 0.79 ± 0.08 | 9.4 ± 0.6 | 0.28 ± 0.01 | 455 ± 3 |
| $TCM_3IPP$ | 0.49 ± 0.01 | 0.45 ± 0.01 | 0.069 ± 0.02 | 0.73 ± 0.3 | 4.4 ± 1.1 | 0.08 ± 0.04 | 219 ± 33 |

[a] Quencher volume fraction was 0.06% volume fraction of PCBM (average of 4–6 measured films). [b] Porphyrin : PCBM blend, weight ratio 1 : 4 (3 device average).

lived singlet excited states thus a decrease in singlet exciton $D$ and $L_D$ is expected. In solution, a significant increase (37–69%) in the generation of singlet oxygen was observed for $TBCM_3PP$ and $TCM_3IPP$ using the quencher 1,3-diphenylisobenzofuran (DBPF) to determine the singlet oxygen quantum yield (Fig. S5†). The increased singlet oxygen generation indicates an increase in the generation of electronic triplet states ($T_1$) caused by high rates of intersystem crossing in the halogen-containing porphyrins.

### c. Preliminary BHJ device studies

Previous studies have shown that in photovoltaic processes short-circuit current density ($J_{sc}$) is correlated with $L_D$; hence an increase in $L_D$ translates into a substantial improvement in energy conversion efficiency.[18,21] Fig. 3 shows the $J$–$V$ curves of $TCM_4PP$, $TBCM_3PP$ and $TCM_3IPP$, and Table 1 lists their photovoltaic characteristics. The open circuit voltage ($V_{oc}$) of the porphyrin devices does not significantly differ between $TCM_4PP$ and $TBCM_3PP$. The energy difference between the highest occupied molecular orbitals (HOMOs) for all the studied porphyrins and lowest unoccupied molecular orbitals (LUMOs) of PCBM are nearly equivalent (Fig. S1/S6†). The lower $V_{oc}$ of $TCM_3IPP$ is an exception because of the low photocurrent density $J_{sc}$ that ultimately limits the obtainable $V_{oc}$.[26] Average $J_{sc}$ values of 0.35, 0.28 and 0.08 mA cm$^{-2}$ were obtained for $TCM_4PP$, $TBCM_3PP$ and $TCM_3IPP$, respectively. The decrease in $J_{sc}$ observed for the heavy atom porphyrin derivatives is correlated to a decrease in $Q$, $D$ and $L_D$ for singlet excitons. The lowered $D$ and $L_D$ suggest that a lower concentration of singlet excitons arrive at the bulk heterojunction interface and dissociate, ultimately decreasing the $J_{sc}$. Although an increase in triplet excitons was observed for the halogen-containing derivatives due to an increased rate of ISC, the porphyrin derivatives used in this study showed a decrease in photoactivity. Possible reasons for the decreased photoactivity include limited triplet exciton diffusion in the porphyrin films or the energetics at the PCBM interface that favor porphyrin triplet state recombination.[50,51] The triplet excited state energy of free-base tetraphenylporphyrins is approximately 1.5 eV.[52] The energy alignment between the porphyrins used in this study and PCBM (Fig. S6†) suggests kinetically lowered and/or thermodynamically unfavorable triplet exciton dissociation at the interface. In addition, triplet excited states that do dissociate at the porphyrin/PCBM interface may be prone to kinetics favoring lowest energy intermolecular charge-transfer (CT) states, ultimately resulting in recombination.[53] Several strategies to enhance the observed photovoltaic performance include utilizing donor and acceptor materials with more favorable energetics for triplet exciton harvesting, device engineering to harvest triplet excited states with co-sensitizers, or the use of triplet exciton blocking layers. Previous work with a Pt porphyrin to enhance photocurrent with triplet excitons utilized a triplet–triplet energy transfer mechanism to a conjugated polymer first, followed by triplet exciton dissociation.[24] In a recent report, the quantum efficiency of a pentacene containing organic solar cell was greatly enhanced by using a triplet exciton blocking poly(3-hexylthiophene) layer.[27] Utilizing these strategies for future work with porphyrin-based OPVs may help to block triplet excitons from diffusing to the anode or suppressing recombination by efficient hole extraction.

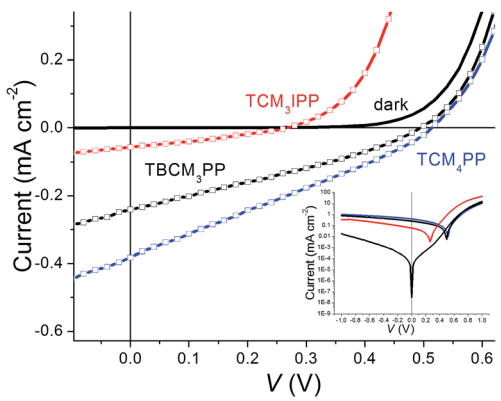


Fig. 3 $J$–$V$ curves of (a) $TCM_4PP$ (—), $TBCM_3PP$ (—) and $TCM_3IPP$ (—) devices blended with PCBM (inset: $J$–$V$ semilog plot).

## Conclusions

The singlet exciton diffusion coefficients and diffusion lengths for solution-cast thin films of metal-free carbomethoxyphenyl porphyrins containing heavy atoms (halogens) have been measured. The decrease in the singlet exciton diffusion length from 15 nm for $TCM_4PP$ to 4.4 nm for $TCM_3IPP$ is proposed to be a consequence of intersystem crossing due to the heavy atom effect. Singlet exciton diffusivity and 3D diffusion lengths were measured by modeling PL decay lifetimes using a Monte Carlo 3D exciton random hopping simulation. The heavy atom effect shortened the singlet excited state lifetime as a consequence of

spin inversion. We therefore observed a decline in $D$, $L_D$, $Q$, and photoactivity with the tetra(carbomethoxyphenyl)porphyrin series. Although the singlet state is effectively quenched using PCBM, the potential to increase triplet state energy generation did not favour improved photoactivity. The energetics at the interface are potentially misaligned for efficient charge generation from the triplet excited state or the device configuration is not an effective architecture to observe triplet state photoconversion efficiency enhancement. It is notable, however, that for these porphyrin systems, good singlet exciton diffusion lengths were measured for thin films of carboxyphenyl porphyrins ($TCM_4PP$ – 15 nm) and the replacement of only one carbomethoxyphenyl group with an iodophenyl group lowers the singlet exciton diffusion length by 71%. This work also demonstrates the usefulness of calculating the 3D exciton diffusion of porphyrin thin films using PL lifetime decay data fit to a simple Monte Carlo model simulation. It is expected that this technique will be useful for measuring the singlet exciton diffusion properties of other porphyrin molecular photoconversion systems.

## Abbreviations

| | |
|---|---|
| OPV | Organic photovoltaic |
| ISC | Intersystem crossing |
| PCBM | [6,6]-Phenyl-C61-butryic acid methyl ester |
| $D$ | Singlet exciton diffusivity |
| $L_D$ | Diffusion length |
| PL | Photoluminescent decay |
| $Q$ | Relative quenching efficiency |
| $J_{SC}$ | Short-circuit current density |
| $V_{OC}$ | Open circuit voltage |
| $TCM_4PP$ | 5,10,15,20-Tetrakis(4-carbomethoxyphenyl) porphyrin |
| $TBCM_3PP$ | 5-(4-Bromophenyl)-10,15,20-tris-(4-carbomethoxyphenyl)porphyrin |
| $TCM_3IPP$ | 5,10,15-Tris-(4-carbomethoxyphenyl)-20-(4-iodophenyl)porphyrin |

## Acknowledgements

This research was funded by the Department of Chemistry at the University of North Carolina at Charlotte, the M.S. Chemistry and Nanoscale Science Ph.D. programs, and through a UNC Charlotte Faculty Research Grant (#111726). J.A.K acknowledges support from the Charlotte Research Scholars (2013) and NSF-REU site program in partnership with the ASSURE program of the DoD (CHE 1156867). M.G.W. acknowledges help with TCSPC and photoluminescence measurements from Prof. Marcus Jones (UNC Charlotte), Gaurav Singh (UNC Charlotte), Sonya Payerpaj (NanoSURE student), and Emily Lam (ACS Project SEED student). The authors acknowledge the use of eDiffusion software provided by Oleksandr Mikhnenko, http://mikhnenko.com/eDiffusion.[39]

## Notes and references

1 T. Fujita, J. C. Brookes, S. K. Saikin and A. N. Aspuru-Guzik, *J. Phys. Chem. Lett.*, 2012, **3**, 2357–2361.
2 J. Huh, S. K. Saikin, J. C. Brookes, S. P. Valleau, T. Fujita and A. N. Aspuru-Guzik, *J. Am. Chem. Soc.*, 2014, **136**, 2048–2057.
3 J. Dostal, T. Mançal, R. Augulis, F. Vacha, J. Psencik and D. Zigmantas, *J. Am. Chem. Soc.*, 2012, **134**, 11611–11617.
4 S. R. Ahrenholtz, C. C. Epley and A. J. Morris, *J. Am. Chem. Soc.*, 2014, **136**, 2464–2472.
5 G. S. Engel, T. R. Calhoun, E. L. Read, T.-K. Ahn, T. Mancal, Y.-C. Cheng, R. E. Blankenship and G. R. Fleming, *Nature*, 2007, **446**, 782–786.
6 M. G. Walter, A. B. Rudine and C. C. Wamser, *J. Porphyrins Phthalocyanines*, 2010, **14**, 759–792.
7 C. Trinh, M. T. Whited, A. Steiner, C. J. Tassone, M. F. Toney and M. E. Thompson, *Chem. Mater.*, 2012, **24**, 2583–2591.
8 T. Kengthanomma, P. Thamyongkit, J. Gasiorowski, A. M. Ramil and N. S. Sariciftci, *J. Mater. Chem. A*, 2013, **1**, 10524–10531.
9 S. M. Khan, M. Kaur, J. R. Heflin and M. H. Sayyad, *J. Phys. Chem. Solids*, 2011, **72**, 1430–1435.
10 G. D. Sharma, D. Daphnomili, S. Biswas and A. G. Coutsolelos, *Org. Electron.*, 2013, **14**, 1811–1819.
11 A. Luechai, J. Gasiorowski, A. Petsom, H. Neugebauer, N. S. Sariciftci and P. Thamyongkit, *J. Mater. Chem.*, 2012, **22**, 23030–23037.
12 C. Reanprayoon, J. Gasiorowski, M. Sukwattanasinitt, N. S. Sariciftci and P. Thamyongkit, *RSC Adv.*, 2014, **4**, 3045–3050.
13 H.-J. Son, S. Jin, S. Patwardhan, S. J. Wezenberg, N. C. Jeong, M. So, C. E. Wilmer, A. A. Sarjeant, G. C. Schatz, R. Q. Snurr, O. K. Farha, G. P. Wiederrecht and J. T. Hupp, *J. Am. Chem. Soc.*, 2012, **135**, 862–869.
14 S. Jin, H.-J. Son, O. K. Farha, G. P. Wiederrecht and J. T. Hupp, *J. Am. Chem. Soc.*, 2013, **135**, 955–958.
15 D. E. Williams, J. A. Rietman, J. M. Maier, R. Tan, A. B. Greytak, M. D. Smith, J. A. Krause and N. B. Shustova, *J. Am. Chem. Soc.*, 2014, **136**, 11886–11889.
16 S. Verma and H. N. Ghosh, *J. Phys. Chem. Lett.*, 2012, **3**, 1877–1884.
17 P. K. B. Palomaki, M. R. Civic and P. H. Dinolfo, *ACS Appl. Mater. Interfaces*, 2013, **5**, 7604–7612.
18 Y. Terao, H. Sasabe and C. Adachi, *Appl. Phys. Lett.*, 2007, **90**, 103515-1–103515-2.
19 T. M. Clarke and J. R. Durrant, *Chem. Rev.*, 2010, **110**, 6736–6767.
20 A. W. Hains, Z. Liang, M. A. Woodhouse and B. A. Gregg, *Chem. Rev.*, 2010, **110**, 6689–6735.
21 S. M. Menke, W. A. Luhman and R. J. Holmes, *Nat. Mater.*, 2013, **12**, 152–157.
22 C.-M. Yang, C.-H. Wu, H.-H. Liao, K.-Y. Lai, H.-P. Cheng, S.-F. Horng, H.-F. Meng and J.-T. Shy, *Appl. Phys. Lett.*, 2007, **90**, 133509.
23 Z. Xu and B. Hu, *Adv. Funct. Mater.*, 2008, **18**, 2611–2617.

 

24 C.-L. Lee, I.-W. Hwang, C. C. Byeon, B. H. Kim and N. C. Greenham, *Adv. Funct. Mater.*, 2010, **20**, 2945–2950.
25 H. Najafov, B. Lee, Q. Zhou, L. C. Feldman and V. Podzorov, *Nat. Mater.*, 2010, **9**, 938–943.
26 A. Kohler and H. Bassler, *Mater. Sci. Eng., Proc. Conf.*, 2009, **66**, 71–109.
27 D. N. Congreve, J. Lee, N. J. Thompson, E. Hontz, S. R. Yost, P. D. Reusswig, M. E. Bahlke, S. Reineke, T. Van Voorhis and M. A. Baldo, *Science*, 2013, **340**, 334–337.
28 G. B. Piland, J. J. Burdett, R. J. Dillon and C. J. Bardeen, *J. Phys. Chem. Lett.*, 2014, **5**, 2312–2319.
29 A. Ormond and H. Freeman, *Materials*, 2013, **6**, 817–840.
30 P. Agostinis, K. Berg, K. Cengel, T. Foster, A. Girotti, S. Gollnick, S. Hahn, M. Hamblin, A. Juzeniene, D. Kessel, M. Korbelik, J. Moan, P. Mroz, D. Nowis, J. Piette, B. Wilson and J. Golab, *Ca-Cancer J. Clin.*, 2011, **61**, 250–281.
31 L. R. Milgrom, *The Colours of Life: An Introduction to the Chemistry of Porphyrins and Related Compounds*, Oxford University Press, New York, 1997.
32 A. Prodi, C. J. Kleverlaan, M. T. Indelli, F. Scandola, E. Alessio and E. Iengo, *Inorg. Chem.*, 2001, **40**, 3498–3504.
33 C. Tanielian and C. Wolff, *J. Phys. Chem.*, 1995, **99**, 9825–9830.
34 E. Azenha, A. C. Serra, M. Pineiro, M. M. Pereira, J. Seixas de Melo, L. G. Arnaut, S. J. Formosinho and A. M. d. A. R. Gonsalves, *Chem. Phys.*, 2002, **280**, 177–190.
35 M. Laranjo, A. C. Serra, M. Abrantes, M. Pineiro, A. C. Goncalves, J. Casalta-Lopes, L. Carvalho, A. B. Sarmento-Ribeiro, A. Rocha-Gonsalves and F. Botelho, *Photodiagnosis Photodyn. Ther.*, 2013, **10**, 51–61.
36 A. C. Serra, M. Pineiro, A. M. d. A. R. Gonsalves, M. Abrantes, M. Laranjo, A. C. Santos and M. F. Botelho, *J. Photochem. Photobiol., B*, 2008, **92**, 59–65.
37 W. Shao, H. Wang, S. He, L. Shi, K. Peng, Y. Lin, L. Zhang, L. Ji and H. Liu, *J. Phys. Chem. B*, 2012, **116**, 14228–14234.
38 M. G. Walter, C. C. Wamser, J. Ruwitch, Y. Zhao, D. Braden, M. Stevens, A. Denman, R. Pi, A. Rudine and P. J. Pessiki, *J. Porphyrins Phthalocyanines*, 2007, **11**, 601–612.
39 O. V. Mikhnenko, H. Azimi, M. Scharber, M. Morana, P. W. M. Blom and M. A. Loi, *Energy Environ. Sci.*, 2012, **5**, 6960–6965.
40 A. Huijser, T. J. Savenije, A. Kotlewski, S. J. Picken and L. D. A. Siebbeles, *Adv. Mater.*, 2006, **18**, 2234–2239.
41 J. D. A. Lin, O. V. Mikhnenko, J. Chen, Z. Masri, A. Ruseckas, A. Mikhailovsky, R. P. Raab, J. Liu, P. W. M. Blom, M. A. Loi, C. J. Garcia-Cervera, I. D. W. Samuel and T.-Q. Nguyen, *Mater. Horiz.*, 2014, **1**, 280–285.
42 O. V. Mikhnenko, J. Lin, Y. Shu, J. E. Anthony, P. W. M. Blom, T.-Q. Nguyen and M. A. Loi, *Phys. Chem. Chem. Phys.*, 2012, **14**, 14196–14201.
43 O. V. Mikhnenko, M. Kuik, J. Lin, N. van der Kaap, T.-Q. Nguyen and P. W. M. Blom, *Adv. Mater.*, 2014, **26**, 1912–1917.
44 A. Huijser, B. M. J. M. Suijkerbuijk, R. J. M. Klein Gebbink, T. J. Savenije and L. D. A. Siebbeles, *J. Am. Chem. Soc.*, 2008, **130**, 2485–2492.
45 H. Donker, A. van Hoek, W. van Schaik, R. B. M. Koehorst, M. M. Yatskou and T. J. Schaafsma, *J. Phys. Chem. B*, 2005, **109**, 17038–17046.
46 A. Huijser, T. J. Savenije, J. E. Kroeze and L. D. A. Siebbeles, *J. Phys. Chem. B*, 2005, **109**, 20166–20173.
47 A. Huijser, T. J. Savenije, S. C. J. Meskers, M. J. W. Vermeulen and L. D. A. Siebbeles, *J. Am. Chem. Soc.*, 2008, **130**, 12496–12500.
48 L. D. A. Siebbeles, A. Huijser and T. J. Savenije, *J. Mater. Chem.*, 2009, **19**, 6067–6072.
49 S. Raisys, K. Kazlauskas, M. Daskeviciene, T. Malinauskas, V. Getautis and S. Jursenas, *J. Mater. Chem. C*, 2014, **2**, 4792–4798.
50 O. V. Mikhnenko, R. Ruiter, P. W. M. Blom and M. A. Loi, *Phys. Rev. Lett.*, 2012, **108**, 137401.
51 C. W. Schlenker, K.-S. Chen, H.-L. Yip, C.-Z. Li, L. R. Bradshaw, S. T. Ochsenbein, F. Ding, X. S. Li, D. R. Gamelin, A. K. Y. Jen and D. S. Ginger, *J. Am. Chem. Soc.*, 2012, **134**, 19661–19668.
52 M. Gouterman and G.-E. Khalil, *J. Mol. Spectrosc.*, 1974, **53**, 88–100.
53 J.-L. Bredas, J. E. Norton, J. Cornil and V. Coropceanu, *Acc. Chem. Res.*, 2009, **42**, 1691–1699.